Atmospheric gaseous elemental mercury (GEM) concentrations and wet and dry deposition of mercury at a high-altitude mountain peak in south China

X. W. Fu[1], X. Feng[1], Z. Q. Dong[2], R. S. Yin[1,3], J. X. Wang[1,3], Z. R. Yang[2], and H. Zhang[1,3]

[1]State Key Laboratory of Environmental Geochemistry, Institute of Geochemistry, Chinese Academy of Sciences, Guiyang 550002, PR China;

[2]Guizhou Environmental Science Research Institute, Guiyang 550002, PR China

[3]Graduate University of the Chinese Academy of Sciences, Beijing 100049, PR China

Correspondence to: X. Feng (fengxinbin@vip.skleg.cn)

Abstract:

China is regarded as the largest contributor of mercury (Hg) to the global atmospheric Hg budget. However, concentration levels and depositions of atmospheric Hg in China are poorly known. Continuous measurements of atmospheric gaseous elemental mercury (GEM) were carried out from May 2008 to May 2009 at the summit of Mt. Leigong in south China. Wet and dry deposition fluxes of Hg were also calculated following collection of precipitation, throughfall and litterfall. Atmospheric GEM concentrations averaged 2.80±1.51 ng m^{-3}, which was highly elevated compared to global background values but much lower than semi-rural and industrial/urban areas in China, indicating great emissions of Hg in central, south and southwest China. Seasonal and diurnal variations of GEM were observed, which reflected variations in source intensity, deposition processes and meteorological factors. Wet deposition of Hg was quite low, while its dry deposition of Hg (litterfall + throughfall-direct wet deposition) constituted a major portion of total deposition (～88% for total mercury (THg) and 84% for methyl mercury (MeHg)). This highlights the importance of vegetation to Hg atmospheric cycling. In a remote forest ecosystem of China, dry deposition of GEM was very important for the depletion of atmospheric Hg. Elevated GEM level in ambient air may accelerate the foliar uptake of Hg through air which may partly explain the elevated Hg dry deposition fluxes observed in Mt. Leigong.

1 Introduction

Mercury (Hg), especially its organic forms (e.g. methylmercury (MeHg) and dimethylmercury (DMeHg)), is a highly toxic pollutant that poses a serious threat to human health and wildlife (National Research Council, 2000). Atmospheric Hg consists of three chemical and physical forms, including gaseous elemental Hg (GEM or Hg^0), divalent reactive gaseous Hg (RGM), and particulate Hg (PHg). Unlike other heavy metals, which tend to exist in the atmosphere in the particulate phase, Hg exists mainly (>95%) in the gaseous phase (total gaseous mercury (TGM), TGM=GEM+RGM) (Schroeder and Munthe, 1998; Poissant et al., 2005; Gabriel et al., 2005; Aspmo et al., 2006; Valente et al., 2007). RGM and PHg are more reactive and readily scavenged via wet and dry deposition. However, GEM, the predominant form of atmospheric Hg (generally constitutes more than 90% the total Hg in atmosphere), is very stable in atmosphere with a residence time between 6 month and 2 years (Schroeder and Munthe, 1998). This enables Hg to undergo a long range transport and makes it well-mixed in a global scale. As such, long range transport of Hg in the atmosphere has been identified as the predominant source of Hg in pristine ecosystem in remote areas.

Wet and dry depositions are very important pathways for scavenging of atmospheric Hg. Because PHg and RGM have the significantly high surface reactivity and water solubility and GEM is very stable in atmosphere, dry and wet deposition of Hg in atmosphere is largely dominated by RGM and PHg. In recently studies, however, dry deposition of atmospheric GEM to forest canopies is increasingly recognized as an important sink for atmospheric Hg. For example, Zhang et al. (2005) reported that the deposition flux of GEM to leaf surface constituted over 99% of total atmospheric Hg loss to vegetation, while St. Louis et al. (2001) and Graydon et al. (2008) found litterfall deposition of Hg constituted about 60% of the total Hg deposition in the forest of experimental lake area (ELA) in Canada . Because Hg adsorbed by root of plant could hardly be translocated from roots to leaf due to the barrier effect of root zone, Hg in leaves should be considered to come from atmosphere (Ericksen et al., 2003; Greger et al., 2005; Selvendiran et al., 2008; Bushey et al., 2008). Therefore, it is reasonable to believe that deposition of GEM to vegetation followed by litterfall deposition is an important sink of atmospheric Hg. Methyl mercury (MeHg) deposition via wet and dry deposition generally constitutes a small portion of

total Hg deposition (Lee et al., 2000; St. Louis et al., 2001). Sources of MeHg in precipitation include capture of MeHg and/or oxidation of dimethyl mercury to MeHg, but the extents of both processes are typically low in the atmosphere (Brosset et al., 1995; Lee et al., 2003).

Since the industrial revolution, global Hg emissions have increased significantly (Fitzgerald, 1995; Mason and Sheu, 2002). In China, many attempts have been made to decrease Hg emissions from coal combustion, smelting activities, cement production, etc. However, China is still regarded as the biggest emission source of atmospheric Hg in the world (Pacyna et al., 2006; Street et al., 2005; Wu et al. 2007). Anthropogenic Hg emissions in China show a clear regional distribution pattern. As shown in Figure 1, central, east and south China are major atmospheric Hg source regions, due to higher population density, proximity to industrial sources and generally higher energy consumption (Street et al., 2005; Wu et al., 2007).

To understand the regional budget of atmospheric Hg and the chemical and physical processes in the atmosphere, it is important to determine spatial and long-tem temporal variability of atmospheric Hg concentrations and deposition fluxes. Numerous studies with regard to atmospheric Hg have been carried out at many sites in North America and Europe (e.g., Poissant et al., 2005; Valente et al., 2007; Sigler et al., 2009; Rutter et al., 2009). However, to the best of our knowledge, only a few long-term monitoring studies of atmospheric Hg and deposition fluxes have been performed in semi-rural and urban/industrial areas of China. Fu et al. (2008a) and Wan et al. (2009a) reported atmospheric TGM concentrations in two semi-rural areas of China (Mt. Gongga in southwest China and Mt. Changbai in northeast China, respectively) which were approximately two times higher than the common background values in North America and Europe (1.5-2.0 ng m^{-3}, Travnikov, 2005; Kim et al., 2005; Valente et al. 2007). In addition, studies in semi-rural and urban areas of China also showed extremely high Hg deposition fluxes (Guo et al., 2008; Wang et al., 2008). These results suggested that many urbanized areas of China are exposed to atmospheric Hg contaminations due to regional anthropogenic emissions. However, there are still restrictions to fully describe temporal and spatial distributions of Hg in China and its relationship to global atmospheric Hg cycling. Hence, there is a great need to conduct long-term continuous measurements of atmospheric Hg and deposition fluxes in remote areas of China.

In this study, we present atmospheric GEM data derived from year-long measurements along with estimates of wet and dry deposition Hg fluxes at a high-altitude mountain peak in remote area

of south China. The major goals of this study are three-fold: 1) to characterize the regional background level of atmospheric GEM as well as wet and dry deposition fluxes of Hg in south China; 2) to evaluate the regional sources and long range transport affecting the GEM concentrations; 3) to discuss the deposition and sink of atmospheric Hg in the forest ecosystem in China.

2 Experiments

2.1 Site description

The sampling site was located at the summit of Mt. Leigong (26.39ºN, 108.20ºE, 2178 m above sea level), which is the highest mountain in southeast Guizhou province in southwest China (Figure 1). Mt. Leigong is an isolated peak with an elevation of about 1000 m in the surrounding landmass. The surrounding areas are naturally preserved semi-tropical evergreen broadleaf forests and semi-tropical deciduous broadleaf and coniferous forests. Mt. Leigong has a subtropical climate, with distinct rainy (May to October) and dry (November to April) seasons. Annual mean air temperature and precipitation depth at the peak of Mt. Leigong are 9 ºC and 1400-1700 mm, respectively. Misty weather prevails at the peak of Mt. Leigong, and the period with clouds generally exceeds 300 days per year.

The sampling site was relatively isolated from human activities; however, several industrial areas and population centers, which might contribute to significant atmospheric Hg release, are located to the west of the sampling site (Figure 1). Guiyang, the capital of Guizhou province, is located about 160 km to the west of the sampling site. The nearest population center is Leishan County (Population: 33,000), which is located 20 km to the southwest but at an elevation of 1300 m below the sampling site. Kaili city, the capital city of the Southeast Guizhou Miao-Dong Autonomous Prefecture, is the biggest population center (population: 520,000) and industrial area in the surrounding area of Mt. Leigong located about 35 km to the northwest of the sampling site.

2.2 Sampling methods and analysis

2.2.1 Measurements of atmospheric GEM

Real time continuous (every 10 minutes) measurements of GEM were made between 9 May 2008 and 18 May 2009 using an automated Hg vapor analyzer (Tekran 2537A) (Lee et al., 1998).

Its technique is based on the collection of TGM (GEM+RGM) on gold traps, followed by thermal desorption, and detection of Hg^0 by cold vapor atomic fluorescence spectrometry (λ=253.7 nm). The instrument features two cartridges which trap gaseous Hg on to gold absorbents. While one cartridge is adsorbing Hg during sampling period, the other is being desorbed thermally and analyzed subsequently for TGM. The functions of each cartridge are then reversed, allowing continuous sampling of ambient air. PHg in ambient air was removed using a 45 mm diameter Teflon filter (pore size 0.2 μm). In this study, the measured TGM concentration was probably dominated by GEM because GEM generally has a concentration level at least two order of magnitude higher than RGM especially in remote areas (Lee et al., 1998, Poissant et al., 2005, Valente et al., 2007; Fu et al., 2008b). Moreover, RGM in ambient air was likely removed when passing the sampling tube, which should have very high humidity in it and was installed with a soda lime before entering the Tekran instrument. Therefore, the atmospheric Hg measured herein was referred to as GEM. Precision (Relative standard deviations) of the sampling system is better than 2% and the absolute detection limit is about 0.1 pg (Tekran, 2002). A Teflon sampling tube with its inlet 8m above the ground was employed at the sampling site. To mitigate the influence of low atmospheric pressure on the pump's strain, a low sampling rate of 0.75 l min^{-1} (at standard temperature and pressure) was used during the whole sampling period. The data quality of Tekran Model 2537A was guaranteed via periodic internal recalibration with a 25 h interval, and the internal permeation source was calibrated every 2 months (after the field measurement study, the external check on the permeation source were within 95.8% (n=5) of expected values).

2.2.2 Sampling method and analysis of precipitation and throughfall

Precipitation samples were collected from May 2008 to May 2009 at an open-air site near the atmospheric TGM sampling site at the peak of Mt. Leigong. To study the dry deposition of Hg to the forest canopy, throughfall samples were simultaneously collected from a Cuculidae forest located within 30 m from the direct wet deposition sampling site. Precipitation and throughfall samples were collected by using a sampler with an acid-washed borosilicate glass bottle and a borosilicate glass wide-mouthed (15 cm in diameter) jar supported in a PVC housing system (developed from Oslo and Paris Commission 1998). Collectors were set out manually just prior or within 15 min of the beginning of a precipitation event. Just following the end of a precipitation event, collectors were sealed using Polyethylene bags to prevent contamination of Hg dry

deposition to the collectors. Precipitation and throughfall samples were both collected weekly throughout the whole study campaign. Each week, samples were transferred carefully to acid-cleaned Teflon sample bottles (volume: 250 mL) and preserved by adding trace-metal grade HCl (to 5‰ of total sample volume). To ensure clean operation, polyethylene gloves were used throughout the setup and collection processes. Teflon bottles with samples were individually sealed into three successive polyethylene bags and rapidly brought to the laboratory and stored in a refrigerator until analysis. Before each of the new sampling cycle, the sampling collectors were rigorously rinsed by Milli-Q water or replaced by new collectors as necessary.

In this study, both total mercury (THg) and methylmercury (MeHg) concentrations in precipitation and throughfall samples were determined following US EPA Method 1631 (US EPA, 1999) and Method 1630 (US EPA, 2001), respectively. THg was analyzed by BrCl oxidation followed by $SnCl_2$ reduction, and dual amalgamation combined with CVAFS detection (US EPA, 1999), while MeHg was determined by using distillation, aqueous phase ethylation and GC separation followed by pyrolysis and GC-CVAFS detection (US EPA, 2001). The detection limits of THg and MeHg were 0.15 ng L^{-1} and 0.03 ng L^{-1}, respectively, which were determined by three times the standard deviation of blanks. Field blanks (n=10) were determined by rinsing the whole sampling collectors with Milli-Q water and then collecting the rinsing water into the 250-mL Teflon bottles as was made for samples to ensure that there was no contamination by sampling collectors, sampling Teflon bottles, and HCl preservative. The overall average THg and MeHg concentrations of field blanks were 0.32 and 0.011 ng L^{-1}, respectively. Precision and accuracy test for the analytical method was made using recoveries on duplicate samples (n=12). The recoveries of THg and MeHg were in the ranges of 96-111% and 95-120%, respectively.

2.2.3 Sampling method and analysis of litterfall

Three typical forests (Cinnamomum camphora (L.) Presl forest, Rhododendron simsii Planch forest, and Fargesia spathacea Franch forest) located at the peak of Mt. Leigong were selected to collect litterfall samples by using three 0.25 m^2 litterfall collectors (St. Louis et al., 2001). Litterfall samples were collected monthly, packed into paper bags and air-dried in a clean environment. Monthly litterfall samples from each site were completely combined to analyze Hg concentrations in litterfall and calculate annual mass flux of each species.

Air-dried litterfall samples were ground to a fine powder in a pre-cleaned food blender and

stored in a clean environment in the laboratory until analysis. During grinding, the blender was extensively cleaned with Mili-Q water and ethanol to prevent any cross contaminations. THg concentrations in litterfall samples were determined by acid digestion followed by oxidation, purge and trap, and cold vapor atomic absorption spectrophotomety (CVAAS). Approximately 0.2 g sample was digested in 10 mL of freshly mixed HNO_3/H_2SO_4 (4:1 v/v) for 6 h at 95 ºC in a water bath. The digested solution was then diluted by adding Mili-Q water to a volume of 50 mL and analyzed for THg. For MeHg analysis, approximately 0.2 g of ground sample was digested for 3 h at 75 ºC in polyethylene bottles containing 5 mL of 25% KOH in methanol (Liang et al., 1996). After cooling to room temperature, MeHg was extracted with methylene chloride and back-extracted from the solvent phase into water, and then the aqueous phase was ethylated for determination of MeHg (Liang et al., 1995, 1996). Quality assurance and quality control were conducted using duplicates, method blanks, matrix spikes, and certified reference material (Tort-2, lobster reference material was used since reference material for plants was not available in our lab). The analytical detection limits were 4 ng g^{-1} for THg and 0.2 ng g^{-1} for MeHg in samples, respectively. Recoveries on matrix spikes of MeHg in samples were in the range of 78-119%. The relative percentage difference was <15% in duplicate samples. An average MeHg concentration of 171±15 ng g^{-1} (n=3) was obtained from Tort-2 which was comparable to the certified value of 152±13 ng g^{-1}.

2.3 Meteorological data and backward trajectory calculation

In this study, wind direction and wind speed were measured using a portable weather station located within 5 m from the TGM sampling site with a time resolution of 30 min. Precipitation depths were measured daily using standard graduated rain gauge, while throughfall depths were obtained by comparing the collected volume with precipitation. Precipitation depth was measured in an open area near its sampling site. The annual precipitation depth from May 2008 to May 2009 was 1533 mm. Throughfall depth was 1182 mm and constituted about 77% (ranging between 60% and 98%) of direct precipitation depth. There was no snow event throughout the sampling campaign because of relative high air temperature and little rainfall in the winter.

In order to identify the long range transport of Hg and its influences on the atmospheric Hg distribution at the study site, three-day back trajectories were calculated using Gridded

Meteorological Data combined with the Geographic Information System (GIS) based software, Trajstat, from HYSPLIT (Wang et al., 2009; http://www.arl.noaa.gov/ready/hysplit4.html). The Global Data Assimilation System (GDAS) meteorological data archives of the Air Resource Laboratory, National Oceanic and Atmospheric Administration (NOAA), which are available on line at (ftp://arlftp.arlhq.noaa.gov/pub/archives/gdas1/) were used as the input. All the back trajectories ended at the sampling site (26.39ºN, 108.20ºE) with an arrival height of 500 m above the ground. The back trajectories were calculated at 6-hour interval (00:00, 06:00, 12:00, 18:00 UTC; i.e. 08:00, 14:00, 20:00, 02:00 local time), and then used for further analysis.

3 Results and discussion

3.1 General characteristics of GEM in atmosphere

Figure 2 shows the time series of 10-min averaged GEM concentrations in ambient air for the entire study period (9 May 2008 to 18 May 2009). The distribution of GEM was characterized by significant variations throughout the sampling campaign. GEM concentrations followed a lognormal distribution pattern (Figure 3), and values between 1.5-4.5 ng m^{-3} accounted for approximately 85% of the total frequency. However, episodes with extremely high GEM concentrations were abundant (0.4% of values were greater than 10 ng m^{-3}), and ~62% of these events was observed in the daytime. These episodes were probably attributed to encounters of air masses from industrial and urbanized areas which probably related to heavily atmospheric Hg pollutions (Kim and Kim, 2001; Liu et al., 2001; Feng et al., 2005). As shown in Sect. 3.4, the sampling site was mainly affected by air masses from regional boundary layer in the daytime and air masses in the free troposphere probably related to long range transport in the night. Considering the site was isolated from industrial actitivities, most of these events were caused by strong Hg sources from industrial and urban areas in the surrounding area in Mt. Leigong whereas others were related to distant sources.

The annual geometric mean of GEM concentrations at the study site was 2.80±1.51 ng m^{-3} and ranged from 0.41 to 23.9 ng m^{-3}, which are much higher than those observed from different remote areas in Europe and North America (generally lower than 2.0 ng m^{-3}, Travnikov, 2005; Kim et al., 2005; Valente et al. 2007). On the other hand, average GEM concentrations in Mt. Leigong are comparable or lower than those observed in remote areas in China and other Asian

countries. The mean TGM concentrations in Mt. Gongga in southwest China and Mt. Changbai in northeast China were 3.98±1.62 ng m^{-3} and 3.58±1.78 ng m^{-3}, respectively (Fu et al., 2008a; Wan et al., 2009a). The level of GEM in Mt. Leigong was within the range (0 to 6.3 ng m^{-3}) measured in the upper troposphere and lower stratosphere around China, Korea and Japan (Friedli et al., 2004), but significantly lower than the levels reported in a Global Atmospheric Watch (GAW) station located on An-Myun Island, Korea (4.61±2.21 ng m^{-3}, Nguyen et al., 2007). Higher GEM levels in China and other countries in East Asia were probably attributed to the large emissions of Hg in these areas in which industries areas and population centers were often densely distributed.

Generally, levels of atmospheric GEM in remote areas are closely related to regional atmospheric Hg emissions. The highly elevated GEM concentrations in rural areas of China probably indicate significant emissions from coal combustion, non-ferrous smelting, cement production, etc. (Pacyna et al., 2006; Street et al., 2005; Wu et al., 2007). However, regional levels of atmospheric GEM in China are not consistent with regional atmospheric Hg emission inventories (Street et al., 2005; Wu et al., 2007). Mt. Changbai and Mt. Gongga are located in northeast China and quaternary section of the eastern Qinghai-Tibet plateau and its transit zone to Sichuan province, respectively, which are within the low atmospheric Hg emission regions in China. However, these two areas showed relatively higher GEM concentrations compared to Mt. Leigong. The major reason for the discrepancy between regional GEM levels and Hg emission inventories is that the sampling sites at Mt. Changbai and Mt. Gongga were affected by regional and local atmospheric Hg emissions (Fu et al., 2008a; Wan et al., 2009a), which probably overestimated the regional backgrounds of atmospheric Hg. In Mt. Gongga, the sampling site was effected by both local domestic Hg emissions and Hg emissions from Zinc and Lead smelting factories in Shimian city located within 50 km from the study site (Fu et al., 2009a), while the sampling site in Mt. Changbai was probably contaminated by local sources because our subsequent measurements in the other site in this area exhibited much lower GEM concentrations (mean: 1.59±0.68 ng m^{-3}, from Oct 2008 to Sep 2009, unpublished data).

3.2 Deposition fluxes of Hg precipitation, throughfall and litterfall

Totally, we collected 32 weekly samples throughout the sampling campaign. We intended to monitor sampling on routine basis; however, interruptions were inevitable for certain periods. The

samples during 23-29 June, 18-24 August and 15-23 September in 2008 were lost during the transport from field to our lab. For the other 19 weeks, sampling was not feasible due to the lack of precipitation. The statistical summaries of the concentrations and fluxes of precipitation, throughfall and litterfall measured at the peak of Mt. Leigong are listed in Table 1. THg concentrations in precipitation samples collected from May 2008 to May 2009 ranged from 1.2 to 30.8 ng L^{-1} (Figure 4), and the overall volume-weighted mean concentration was 4.0 ng L^{-1}. By comparison, THg concentrations in all throughfall samples throughout the period were higher than precipitation levels (Figure 4). The annual volume-weighted mean THg concentration for throughfall was 8.9 ng L^{-1} with a range of 2.8 - 32.5 ng L^{-1}. In general, vegetation is a sink for atmospheric Hg (Erichsen et al., 2003; Bushey et al., 2008). Zhang et al. (2005) and Poissant et al. (2008) found that foliage was a sink of all atmospheric Hg species and deposition of atmospheric Hg to foliar surfaces are enhanced as atmospheric Hg concentrations increased. Generally, both stomatal and nonstomatal pathways are important ways for atmospheric Hg to enter vegetation leaves (Stamenkovic and Gustin, 2009). However, not all atmospheric Hg deposited to the foliar surface is assimilated and fixed by foliage, and most of the PHg and RGM are probably washed off the leaf surface or reduced and then reemitted to the atmosphere (Rea et al., 2001). Therefore, elevated THg concentration in throughfall was mostly attributed to the dry deposition of PHg and RGM to vegetation followed by washout of throughfall.

MeHg concentrations in precipitation ranged from below the detection level to 0.15 ng L^{-1} with a volume-weighted concentration of 0.04 ng L^{-1}. Like THg, MeHg in throughfall was elevated compared to direct precipitation; MeHg in throughfall ranged from 0.02-0.40 ng L^{-1} and the volume-weighted mean was 0.10 ng L^{-1}. This was probably due to dry deposition of MeHg to foliage. The average fractions of THg present as MeHg in precipitation and throughfall were 1% and 1.1%, respectively, which were comparable or lower than values reported for Europe and North America (Porvair and Verta, 2003; Hall et al., 2005; Witt et al., 2009), as well as an upland forest in Mt. Gongga in southwest China (Fu et al., 2009b).

Concentrations of THg and MeHg in litterfall were highly variable and ranged from 57-110 and 0.44-0.80 ng g^{-1}, respectively. The distribution of THg in litter types was consistent with MeHg. The lowest THg and MeHg concentrations were measured in Rhododendron simsii Planch, whereas the concentrations levels in the other two litter types were comparable. The fractions of

Hg present as MeHg in throughfall samples ranged from 0.65 to 0.77%, which are lower than those of direct precipitation and throughfall. This suggests that uptake of MeHg from precipitation by foliage is relatively small.

THg and MeHg concentrations in precipitation and throughfall in the study area were considerably lower than those reported in rural and semi-rural areas of China (Fu et al., 2009b; Guo et al., 2008; Wang et al., 2009; Wan et al., 2009b). This is because the sampling site was isolated from sites near human activities. However, it is interesting that THg and MeHg concentrations in Mt. Leigong were comparable or lower than those reported in North America and Europe (Schwesig and Matzner, 2000; St. Louis et al., 2001; Hall et al., 2005; Choi et al., 2008; Witt et al., 2009). This is quite different from atmospheric GEM concentrations, which were elevated compared to sites in Europe and North America. This result suggests that atmospheric GEM had less immediate effect on direct wet deposition and throughfall compared to PHg and RGM. Since the study site was not a durably impacted receptor for direct anthropogenic Hg emission sources, the likelihood for steadily elevated RGM and PHg levels here are limited. These airborne fractions are transients in atmospheric boundary layer and have a limited role in the corresponding long-range transport. Although not measured, we may therefore speculate that the contribution of RGM and PHg to airborne Hg levels and deposition fluxes at Mt Leigong is restricted. On the other hand, GEM could undergo long range transport from emission sources and cause elevated levels at the sampling site. This may explain the low precipitation THg concentrations and high atmospheric GEM concentrations in Mt. Leigong.

Besides, precipitation THg concentration at the peak of Mt. Leigong was also significantly lower compared to a nearby site (within 10 km) (19.5 ng L^{-1}, Wang et al., 2009) located at a lower elevation (1400 m above sea level), indicates that there is a significant difference in the source of rain because of mountain climate or that wash out of atmospheric Hg during a rain event constitutes a major portion of wet deposition compared to cloud process. THg concentrations in litterfall at Mt. Leigong were much higher than those from North America and Europe (Schwesig and Matzner, 2000; St.Louis et al., 2001; Hall and St.Louis et al., 2004; Sheehan et al., 2006), which was consistent with results for atmospheric GEM. This may suggest that Hg content in vegetation leaf was significantly related to atmospheric GEM concentration.

Fluxes of THg and MeHg in precipitation and throughfall were estimated using the

volume-weighted concentrations and depths of precipitation and throughfall, and litterfall deposition fluxes of THg and MeHg were estimated using the litterfall Hg concentrations and litter mass fluxes. The annual THg deposition flux was 6.1 μg m^{-2} yr^{-1} for direct precipitation, 10.5 μg m^{-2} yr^{-1} for throughfall and 39.5 μg m^{-2} yr^{-1} for litterfall. The annual MeHg deposition flux was 0.06 μg m^{-2} yr^{-1} for direct precipitation, 0.12 μg m^{-2} yr^{-1} for throughfall and 0.28 μg m^{-2} yr^{-1} for litterfall. Net throughfall (throughfall-precipitation) and litterfall had been suggested to be a good pathway to estimate dry deposition of atmospheric Hg (St.Louis et al., 2001; Rea et al., 2001; Graydon et al., 2006; Graydon et al., 2009). The annual dry deposition fluxes of THg and MeHg were estimated to be 43.9 and 0.34 μg m^{-2} yr^{-1}, respectively. Obviously, dry deposition flux played the dominant role in atmospheric Hg deposition, and constituted 88% for total THg deposition and 85% for total MeHg deposition, respectively. It should be noted that our estimate of dry deposition is subjected to some uncertainties. Graydon et a. (2009) discussed the influence of reemission of Hg previously deposited to foliage on the estimate of dry deposition of THg using net throughfall and litterfall method and found the dry deposition flux could be underestimated 3-5%. Moreover, dry deposition of Hg to soil was not calculated in this study due to the lack of soil/air flux measurement. Since the exchange of Hg between forest soil and atmosphere generally exhibits the bio-directional pattern (Kim et al., 1995; Feng et al., 2005; Fu et al., 2008c), the estimation of THg dry deposition is probably underestimated because the dry deposition of Hg to forest soil was not included. The uncertainty for the estimation of MeHg dry deposition was probably higher than THg, and this could be caused by many factors as those described below. Firstly, there is still not enough evidence supporting that the atmosphere MeHg is the exclusive source of MeHg in vegetation leaf, and this might overestimate the atmospheric MeHg dry deposition flux using litterfall method. Besides, reemission of MeHg from foliar surface and exchange flux of MeHg between forest soil and atmosphere would also cause uncertainties (unfortunately there is still lack of such information).

Dry deposition of THg in the forest area of Mt. Leigong was much higher than values observed from forests in North America and Europe (Grigal et al., 2000; Lee et al., 2000; Larssent et al., 2008; Graydon et al., 2009). We attributed this to the high GEM concentrations in the study area. As suggested by Zhang et al. (2005) and Poissant et al. (2008), atmospheric Hg^0 is almost the exclusive source of Hg in vegetation leaf. Highly elevated litterfall deposition fluxes suggests that

in remote forest areas of China, deposition of atmospheric Hg^0 via uptake by vegetation leaf was the major pathway for the depletion of atmospheric Hg. Moreover, the great deposition via litterfall also constituted an very important source of Hg in forest ecosystem of China. Previous study by Obrist (2007) suggested that Hg deposited to forest might be probably reemitted to atmosphere during carbon mineralization. Our study in the upland forest of Mt. Gongga (2500 m above sea level) found that emission of Hg from litterfall (the sampling site was covered by 1-2 cm undecomposed leaf litter. Mean flux was 0.5 ng m^{-2} h^{-1} in Aug 2006) was much lower compared to bare soil (Fu et al., 2008c). Using this data, the annual emission flux of litterfall in Mt. Leigong was calculated to be 4.4 μg m^{-2} yr^{-1}, (which was probably overestimated because evasion of Hg from litter in cold season was probably lower than the values in warm season), indicating that the reemission during litter decomposition was very small and most of the Hg in litter probably retained in the forest soil.

3.3 Seasonal variation of atmospheric GEM and Hg deposition fluxes

Monthly geometric mean GEM concentrations in Mt. Leigong are shown in Figure 5A. GEM concentrations showed a clear seasonal cycle with high concentrations in cold seasons and low concentrations in warm seasons. The lowest monthly geometric mean GEM concentration (1.52±1.06 ng m^{-3}) was observed in July 2008, and then increased consistently and reached the highest monthly value (4.42±0.95 ng m^{-3}) in January 2008, which was nearly threefold higher than that in July 2008. The seasonal variation of GEM concentrations was in the descending order of winter, spring, autumn and summer (Table 2).

Low summer concentrations and elevated winter concentrations were reported for south and southwest China (Feng et al., 2004; Fu et al., 2008a). A previous study in the Mt. Gongga area suggested enhanced coal and biomass combustion played a significant role in elevated TGM concentrations in cold season (Fu et al., 2008a; Fu et al., 2009a). Enhanced coal and biomass combustion in cold seasons is generally driven by the need for residential heating in China. Compared to industrial and urban areas in which the coal consumption is dominated by industrial and power plant activities which are often evenly distributed in each month, the increase of coal consumption in Mt. Leigong area in cold seasons could be more significant because domestic use of coal is dominant. This was probably one of most important reasons for the highly elevated

GEM concentrations in Mt. Leigong in cold seasons. Moreover, the seasonal variability may also be due to long range transport of atmospheric Hg during monsoons. In cold seasons, the wind field in the study area was dominated by winter monsoons, which originated from or passed through central China (Figure 6A), one of the most Hg-polluted regions in China (Street et al., 2005; Wu et al., 2007). The air masses would probably capture a large amount of Hg during transport and cause elevated GEM concentrations in cold seasons. In the warm season, air masses originating from the ocean dominated, although sometimes the inland air masses occasionally affected the study site (Figure 6B). Marine air masses in warm seasons likely diluted the atmospheric Hg in the study area.

Wet deposition fluxes of THg and MeHg also showed clear seasonal variations (Figure 5B). The seasonal distribution pattern for both THg and MeHg fluxes were in the descending order: summer > spring > autumn > winter (Table 2). The highest monthly THg wet deposition flux of 1573 ng m^{-2} mon^{-1} was observed in August 2008, while the lowest monthly mean of 66 ng m^{-2} mon^{-1} was observed in October 2008. The monthly variation of MeHg wet deposition fluxes differed from THg, with the highest monthly mean of 14.4 ng m^{-2} mon^{-1} observed in May 2008 and the lowest monthly mean of 0.5 ng m^{-2} mon^{-1} observed in March 2009. Correlation analysis between wet deposition fluxes of THg and MeHg and precipitation depths indicated that wet deposition fluxes were positively correlated with precipitation depths (r_{THg}=0.77, r_{MeHg}=0.36, $P<0.01$).

Seasonal variation of dry deposition fluxes of Hg is difficult to quantify. Net throughfall fluxes of THg varied seasonally in the descending order of summer, spring, winter and autumn, while the seasonal variation of MeHg was in the descending order of spring, autumn, summer and winter. However, as discussed in section 3.2, litterfall was the dominant pathway for dry deposition. It is very difficult to predict the seasonal variation of litterfall deposition fluxes because vegetation will not immediately fall off after the uptake of atmospheric Hg. However, growing seasons for vegetation in the study area are generally between late April and later October, in which vegetation could increase dry deposition of atmospheric Hg via foliage uptake. Therefore, it is reasonable to predict dry deposition of atmospheric Hg was probably higher in warm seasons than that in cold seasons.

3.4 Diurnal variation of atmospheric GEM

GEM concentrations in Mt. Leigong exhibited a noticeable diurnal pattern as shown in Figure 7. GEM concentrations decreased consistently from mid-night (at 0:00 in China central time (CCT)) to 2.5-2.6 ng m^{-3} at 05:30, and remained at this level for about 2 hours until 07:30. After sunrise, GEM concentrations increased quickly to 2.9-3.0 ng m^{-3} at 12:00 and remained constant until 16:00. After that, GEM concentrations decreased consistently to the lowest values before sunrise.

The diurnal distribution of GEM in Mt. Leigong gives insight into the interplay of regional emissions and long range transport of Hg influencing the GEM concentrations. Since the sampling site was located at the peak of Mt. Leigong, mountain valley breezes played a significant role in the wind direction. During the daytime, the air mass in the low altitude area of Mt. Leigong is heated because of increasing solar radiation, resulting in an upslope flow that brings air from the boundary layer to the mountain peak; while at night, air adjacent to mountain peak cools faster than air in the low altitude area, causing a reversal flow (downslope), which enables transport of air masses from the free troposphere to the sampling site. It is clear that air masses from the boundary layer and the free troposphere both showed elevated GEM concentrations compared to background values in Northern hemisphere (Travnikov, 2005; Kim et al., 2005; Valente et al. 2007). Relatively higher GEM concentrations in air masses from boundary layer indicated a large amount of atmospheric Hg emission in the surrounding areas of Mt. Leiong. The elevated GEM concentrations in the free troposphere were probably caused by the updraft, which carried polluted air masses from the boundary layer. On the other hand, since the air masses in the free troposphere have a higher velocity (Figure 7), the highly Hg polluted air in south China could probably be transported long distances and caused pollution problems in other regions.

3.5 Sources identification of atmospheric Hg at the study site

Figure 8A shows wind roses at the sampling site, which indicated wind directions at the study site were dominantly from northeast, southeast and southwest, which may reflect the three predominant monsoons in China including Southeast monsoon, Southwest monsoon and Asian winter monsoon. Distributions of GEM concentrations in each of the wind direction were quite different from each other. In general, northeast wind and southwest wind exhibited higher GEM

events, while southeast wind exhibited lower GEM events. Wind dependence of atmospheric GEM was probably attributed to an interplay of regional sources and long range transport of Hg.

3.5.1 Regional sources

As discussed in section 3.4, the sampling site was dominantly affected by the valley wind during the daytime, which transported regional air masses from the boundary layer. To gain a better understanding of the influences of regional sources on GEM distributions in Mt. Leigong, daytime GEM dependence on wind direction is shown in Figure 8B. In general, high mean GEM concentrations were observed mostly from west, and this indicates the influence from regional sources in this direction. Due to high coal Hg content, non-ferrous smelting activities and artisanal Hg mining activities, Guizhou is regarded as one of the highest atmospheric Hg source regions in China (Street et al., 2005; Wu et al., 2007; Feng and Qiu, 2008; Li et al., 2009). Kaili (located 35 km northwest of Mt. Leiong) is the largest city in the study area, and may be affected by elevated Hg emissions (Liu et al., 2002; Feng et al., 2004). Besides, several smelting factories were located around the city. Therefore, it is an important regional source for the study area. Leishan (20 km southwest of Mt. Leigong) is the nearest population centre of the study site, which is also an important source region influencing the study site. Moreover, the densely populated areas and industrial areas were located to the west of the sampling sites, which definitely contributed to the elevated concentrations in this direction.

Except for the northeast direction which was probably affected by the artisanal Hg mining activities in Tongren city (Li et al., 2009), air flow from the east and south showed low GEM levels. The lowest mean GEM concentrations were observed from the southeast direction, which was probably because this area is more naturally preserved and less populated.

3.5.2 Air mass back trajectories analysis for long range transport

In order to gain an insight to the influence of long range transport on distribution of GEM in Mt. Leigong, we calculated 3-day air mass back trajectories using the Gridded Meteorological Data combined with the free software Trajstat from HYSPLIT website (Wang et al., 2009; *http://www.arl.noaa.gov/ready/hysplit4.html*). The 3-day back trajectories arriving at the study site over the study period were grouped into four clusters, which are shown in Figure 9. Cluster 1 consists of air masses originating from the continental inland areas of central Asia, passing over the north and central China. Cluster 2 shows air masses originated from south China. Air masses

in cluster 3 were originated from South China Sea, then passed over Guangxi province. Cluster 4 shows air masses originated from southwest China and then passed over Guizhou province.

Contributions of the above four types of air masses were quite different throughout the year. Cluster 1 had the highest frequency (50.8%) of all the four groups, while cluster 4 contributed least (4.6%) to the total air masses (Figure 9). Frequencies of cluster 2 and 3 were 22.1% and 22.5%, respectively. For the four types of air masses, cluster 1 was related to the highest GEM concentrations (3.49 ng m^{-3}). Air masses in cluster 1 passed over the central China plain region, which is the most densely populated and heavily Hg polluted area in China due to industrial and domestic coal combustion, smelting industries, cement production, biomass burning, etc. For example, Henan and Hunan provinces were the first and fourth biggest Hg source provinces in China (Wu et al., 2007), respectively, which together accounted for about 15% of the total Hg emissions. Highly elevated GEM concentrations, together with the highest occurrence, may be an important reason for elevated GEM level in Mt. Leigong. Mean GEM concentration in cluster 2 was 2.73 ng m^{-3}, which was considerably lower compared to cluster 1. This is probably because the air masses originated or passed over the border area of the three provinces of Guangdong, Guangxi and Hunan, which is generally less populated and less developed. Air masses in cluster 3 showed the lowest mean GEM concentration of 2.12 ng m^{-3}, which was probably attributed to the oceanic origins of these air masses. Air masses in cluster 4 were also heavily polluted with regard to Hg, with a mean concentration of 3.46 ng m^{-3}, comparable to cluster 1 result. This result might be explained by the elevated Hg emissions in Guizhou province, the second biggest atmospheric Hg source region in China.

In general, GEM distribution in the study area was controlled by Hg emissions in the regional boundary layer and Hg levels in the free troposphere which were probably related to well-mixed long range transport air masses. As discussed in sect. 3.4, the sampling site was affected by the alternation of mountain breeze and valley breeze, which were probably related to long range transport and regional Hg sources, respectively. Using the lowest GEM concentrations in the night and highest concentrations in the daytime, we could simply speculate that the levels of GEM in regional boundary layer and well-mixed long range transport air masses in the free troposphere (assuming to be the regional base-case level) were about 2.94 (mean GEM concentration between 12:00 and 16:00 in the daytime) and 2.56 ng m^{-3} (mean GEM concentration between 5:30 and 7:30

in the night), respectively. the high GEM concentration (~0.38 ng m^{-3} higher than regional base-case concentration) in regional boundary layer indicates that regional Hg emissions played an important role in Mt. Leigong. However, it should be pointed out that the GEM concentration in well-mixed long range transported air masses in the free troposphere was elevated by ~1.0 ng m^{-3} compared to background values in the northern hemisphere (assuming to be 1.5 ng m^{-3}). Therefore, we suggest that long range transport played a more significant role in Mt. Leigong compared to regional sources.

4. Summary and conclusions

Measurements of GEM in ambient air and wet and dry deposition fluxes were investigated at Mt. Leigong, a high-altitude peak in south China from May 2008 to May 2009. Atmospheric GEM levels were highly elevated compared to background values observed in the northern hemisphere (1.5-2.0 ng m^{-3}) with an overall geometric mean concentration of 2.80 ng m^{-3}. A distinct seasonal distribution pattern was observed with GEM concentrations with higher levels in winter and lower levels in summer, and this was probably attributed to seasonal variations in anthropogenic emission sources, meteorological conditions and atmospheric scavenging processes (transformation and deposition). Diurnal variations in GEM concentrations were observed with higher concentrations in the daytime and lower levels at night and were likely due to mountain valley breeze circulation. The prevalent valley wind during the daytime carried polluted air masses from regional boundary layer and increased GEM levels at the sampling site, while during the night the sampling site was mainly infused with mountain wind which carried fresh air from free troposphere.

Annual means of THg and MeHg concentrations in direct wet deposition were 4.0 and 0.04 ng L^{-1}, respectively. THg and MeHg concentrations in throughfall were more than twofold higher than direct wet deposition, with the annual means of 8.9 and 0.10 ng L^{-1}, respectively. Even through Mt. Leigong was highly polluted with atmospheric GEM, annual wet deposition fluxes of THg (6.1 μg m^{-2} yr^{-1}) and MeHg (0.61μg m^{-2} yr^{-1}) were comparable or lower compared to those reported in Europe and North America, indicating GEM in atmosphere was not the immediate factor influencing wet deposition. Dry deposition fluxes of THg (43.9 μg m^{-2} yr^{-1}) and MeHg (0.34 μg m^{-2} yr^{-1}) in Mt. Leigong were much higher compared to wet deposition, which were

estimated via net throughfall fluxes (annual mean for THg: 4.4 μg m^{-2} yr^{-1}, MeHg: 0.06 μg m^{-2} yr^{-1}) together with litterfall fluxes (annual mean for THg: 39.5 μg m^{-2} yr^{-1}, MeHg: 0.28 μg m^{-2} yr^{-1}). The elevated dry deposition of THg in Mt. Leigong was predominantly attributed to the elevated GEM concentrations, which could be adsorbed by vegetation foliage. Our study indicated that dry deposition of GEM was the dominant pathway for Hg entering remote forest ecosystem, whereas RGM and PHg emitted from industrial sources were locally deposited because of high surface reactivity and water solubility.

The study site was affected by both regional emissions and long range transport of Hg. Regional emissions of Hg included coal combustion and smelting activities which were generally located in the west of Mt. Leigong. Our results indicate Mt. Leigong may be affected by both continental inland monsoon and Southeast monsoon, which carried Hg polluted air masses from central China and Guizhou province, whereas air masses from south China were generally related to low atmospheric Hg concentrations because of oceanic flow.

Acknowledgements. This work is supported by the Sino-Norwegian cooperation Project: "Capacity building for reducing mercury pollution in China-Case Study in Guizhou province" which was funded by the Norwegian Government, and Natural Science Foundation of China (40721002) with additional support from the Startup Funds for the Chinese Academy of Science Dean's Reward. We also thank the staff of Leishan County Forestry Administration for field sampling assistance.

References

Aspmo, K., Temme, C., Berg, T., Ferrari, C., Gauchard, P. A., Fain, X., and Wibetoe, G.: Mercury in the atmosphere, snow and melt water ponds in the North Atlantic Ocean during Arctic summer, Environ. Sci. Technol., 40, 4083-4089, 2006.

Brosset, C., and Lord, E.: Methylmercury in ambient air, Method of determination and some measurement results, Water Air Soil Poll. 82, 739-750, 1995.

Bushey, J. T., Mallana, A. G., Montesdeoca, M. R., and Driscoll, C. T.: Mercury dynamics of a northern hardwood canopy, Atmos. Environ., 42, 6905-6914, 2008.

Choi, H. D., Sharac, T. J., and Holsen, T. M.: Mercury deposition in the Adirondacks: A comparison between precipitation and throughfall, Atmos. Environ., 42, 1818-1827, 2008.

Erichsen, J. A., Gustin, M. S., Schorran, D. E., Johnson, D. W., Lindberg, S. E., and Coleman, J. S.: Accumulation of atmospheric mercury in forest foliage, Atmos. Environ., 37, 1613-1622, 2003.

Feng, X., Shang, L., Wang, S., Tang, S., and Zheng, W.: Temporal variation of total gaseous mercury in the air of

Guiyang, China, J. Geophys. Res., 109:D03303. doi:10.1029/2003JD004159, 2004.

Feng, X., Wang, S., Qiu, G., Hou, Y., Tang, S.: Total gaseous mercury emissions from soil in Guiyang, Guyizhou, China, J. Geophys. Res., 110: D14306, doi:10.1029/2004JD005643, 2005.

Feng, X., Qiu, G.: Mercury pollution in Guizhou, China- an overview. Sci. Total Environ., 400, 227 − 237, 2008.

Fitzgerald, W. F.: Is mercury increasing in the atmosphere? The need for an atmospheric mercury network (AMNET), Water Air Soil Pollut., 80, 245–254, 1995.

Friedli, H. R., Radke, L. F., Prescott, R., Li, P., Woo, J. H., and Carmichael, G. R.: Mercury in atmosphere around Japan, Korea and China as observed during the 2001 ACE-Asia field campaign: Measurements, distributions, sources, and implication, J. Geophys. Res., 109, D19S25, doi:10.1029/2003JD004244, 2004.

Fu, X. W., Feng, X. B., Zhu, W. Z., Wang, S. F., and Lu, J.: Total gaseous mercury concentrations in ambient air in the eastern slope of Mt. Gongga, South-Eastern fringe of the Tibetan plateau, China, Atmos. Environ., 42, 70–979, 2008a.

Fu, X. W., Feng, X. B., Zhu, W. Z., Zheng, W., Wang, S. F., Lu, J. Y.: Total particulate and reactive gaseous mercury in ambient air on the eastern slope of the Mt. Gongga area, China, Appl. Geochem., 23, 408-418, 2008b.

Fu, X. W., Feng, X. B., and Wang, S. F.: Exchange fluxes of Hg between surfaces and atmosphere in the eartern flank of Mount Gongga, Sichuan province, southwestern China, J. Geophys. Res., 113, D20306, doi:10.1029/2008JD009814, 2008c.

Fu, X. W., Feng, X. B., Wang, S. F., Rothenberg, S., Shang, L. H., Li, Z. G., and Qiu, G.L.: Temporal and spatial distributions of total gaseous mercury concentrations in ambient air in a mountainous area in southwestern China: Implications for industrial and domestic mercury emissions in remote areas in China, Sci Total Environ., 407, 306-2314, 2009a.

Fu, X. W., Feng, X. B., Zhu, W. Z., Rothenberg, S., Yao, H., Liu, N., and Yin, R. S.: Elevated atmospheric deposition and dynamics of mercury in a remote upland forest of Southwestern China, Environ. Pollut., in review, 2009b.

Gabriel, M. C., Williamson, D. G., Brooks, S., and Lindberg, S.: Atmospheric speciation of mercury in two contrasting Southeastern US airsheds, Atmos. Environ., 39, 4947-4958, 2005.

Grigal, J. A., Kolka, R. K., Fleck, J. A., and Nater, E. A.: Mercury budget of an upland-peatland watershed, Biogeochemistry, 50, 95-109, 2000.

Graydon, J. A., St. Louis, V. L., Lindberg, S. E., Hintelmann, H., and Krabbenhoft, D. P.: Investigation of mercury exchange between forest canopy vegetation and the atmosphere using a new dynamic chamber, Environ. Sci. Technol., 40, 4680-4688, 2006.

Graydon, J. A., St. Louis, V. L., Hintelmann, H., Lindberg, S. E., Sandilands, K. A., Rudd, J. W. M., Kelly, G. A., Hall, B. D., and Mowat, L. D.: Long-term wet and dry deposition of total and methyl mercury in the remote boreal ecoregion of Canada, Environ. Sci. Technol., 42, 8345-8351, 2009.

Greger, M., Wang, Y., and Neuschulz, C.: Absence of Hg transpiration by shoot after Hg uptake by roots of six

terrestrial plant species, Environ. Pollut., 134(2), 201–208, 2005.

Guo, Y. N., Feng, X. B., Li, Z. G., He, T. R., Yan, H. Y., Meng, B., Zhang J. F., and Qiu, G. L.: Distribution and wet deposition fluxes of total and methyl mercury in Wujiang reservoir Basin, Guizhou, China, Atmos. Environ. 42, 7096-7103, 2008.

Hall, B. D., and St. Louis, V. L.: Methylmercury and total mercury in plant litter decomposing in upland forests and flooded landscapes, Environ. Sci. Technol., 38, 5010-5021, 2004.

Hall, B. D., Manolopoulos, H., Hurley, J. P., Schauer, J. J., St. Louis, V. L., Kenski, D., Graydon, J., Babiarz, C. L., Cleckner, L. B., and Keeler, G. J.: Methyl and total mercury in precipitation in the Great Lakes region, Atmos. Environ., 39, 7557-7569, 2005.

Kim, K. H., Lindberg, S. E., and Meyers, T. P.: Micrometeorological measurements of mercury vapor fluxes over background forest soils in eastern Tennessee, Atmos. Environ., 29, 267-282, 1995.

Kim, K. H., and Kim, M. Y.: The temporal distribution characteristics of total gaseous mercury at an urban monitoring site in Seoul during 1999-2000, Atmos. Environ., 35, 4253-4263, 2001.

Kim, K. H., Ebinghaus, R., Schroeder, R., Blanchard, P., Kock, H. H., Steffen, A., Froude, F. A., Kim, M. Y., Hong, S. M., and Kim, J. H.: Atmospheric mercury concentrations from several observatory sites in the northern hemisphere, J. Atmos. Chem., 50, 1-24, 2005.

Larssen, T., de Wit, H. A., Wiker, M., and Halse, K.: Mercury budget of a small forested boreal catchment in southeast Norway, Sci. Total Environ., 404, 290-296, 2008.

Lee, D. S., Dollard, G. J., and Pepler, S.: Gas-phase mercury in the atmosphere of the United Kingdom, Atmos. Environ., 32, 855-864, 1998.

Lee, Y. H., Bishop, K. H., and Munthe, J.: Do concepts about the catchment cycling of methylmercury and mercury in boreal catchments stand the test of time? Six years of atmospheric inputs and runoff export at Svartberget, northern Sweden, Sci. Total Environ., 260, 11-20, 2000.

Li, P., Feng, X. B., Shang, L. H., Qiu, G. L., Meng, B., Liang, P., and Zhang H.: Mercury pollution from artisanal mercury mining in Tongren, Guizhou, China, Atmos. Environ., 23, 2055-2064, 2009.

Liang, L., Horvat, M., and Danilchik, P.: A novel analytical method for determination of picogram levels of total mercury in gasoline and other petroleum based products, Sci. Total Environ., 187, 57-64, 1995.

Liang, L., Horvat, M., Cernichiari, E., Gelein, B., and Balogh, S.: Simple solvent extraction technique of elimination of matrix interferences in the determination of methylmercury in environmental and biological samples by ethylation-gas chromatography– cold vapor atomic fluorescence spectrometry, Talanta, 43, 1883–1888, 1996.

Liu, S. L., Nadim, F., Perkins, C., Carley, R. J., Hoag, G. E., Lin, Y. H., and Chen, L. T.: Atmospheric mercury monitoring survey in Beijing, China, Chemos., 48, 97–107, 2002.

Lee, Y. H., Bishop, K. H., and Munthe, J.: Do concepts about catchment cycling of methylmercury and mercury in boreal catchments stand the test of time? Six years of atmospheric inputs and runoff export at Svartberget, northern Sweden, Sci. Total Environ., 260, 11-20, 2000.

Lee, Y. H., Wangberg, I., and Munthe, J.: Sampling and analysis of gas-phase methylmercury in ambient air, Sci. Total Environ., 304, 107-113, 2003.

Mason, R. P. and Sheu, G.-R.: Role of the ocean in the global mercury cycle, Global Biogeochem. Cy., 16, 1093, doi:10.1029/2001GB001440., 2002.

National Research Council: Toxicological effects of MeHg, Committee Report, Board of Environmental Studies and Toxicology, National Academy press, Washing DC, P. 344, 2000.

Nguyen, H. T., Kim, K. H., Kim, M. Y., Hong, S. M., Youn, Y. H., Shon, Z. H., and Lee, J. S.: Monitoring of atmospheric mercury at a Global Atmospheric Watch (GAW) site on An-Myun, Island, Korea, Water Air Soil Pollut., 185, 149-164, 2007.

Obrist, D.: Atmospheric mercury pollution due to losses of terrestrial carbon polls? Biogeochemistry, 85, 119-123, 2007.

Oslo and Paris Commission: JAMP guidelines for the sampling and analysis of mercury in air and precipitation, Joint assessment and monitoring programme, pp. 1-20, 1998.

Pacyna, E. G., Pacyna, J. M., Steenhuisen, F., and Wilson, S.: Global anthropogenic mercury emission inventory for 2000, Atmos. Environ., 40, 4048-4063, 2006.

Poissant, L., Pilote, M., Beauvais, C., Constant, P., and Zhang, H. H.: A year of continuous measurements of three atmospheric mercury species (GEM, RGM and Hg–P) in southern Québec, Canada, Atmos. Environ., 39, 1275–1287, 2005.

Poissant, L., Pilote, M., Yumvihoze, E., and Lean, D.: Mercury concentrations and foliage/atmosphere fluxes in a maple forest ecosystem in Québec, Canada, J. Geophys. Res., 113, D10307, doi:10.1029/2007JD009510, 2008.

Porvari, P., and Verta, M.: Total and methyl mercury concentrations and fluxes from small boreal forest catchments in Finland, Environ. Pollut. 123, 181-191, 2003.

Rea, A. W., Lindberg, S. E., and Keeler, G. J.: Dry deposition and foliar leaching of mercury and selected trace elements in deciduous forest throughfall, Atmos. Environ., 35, 3453-3462, 2001.

Rutter, A. P., Snyder, D. C., Stone, E. A., Schauer, J. J., Gonzalez-Abraham, R., Molina, L. T., Márquez, C., Cárdenas, B., and de Foy, B.: In situ measurements of speciated atmospheric mercury and the identification of source regions in the Mexico City Metropolitan Area, Atmos. Chem. Phys., 9, 207-220, 2009, http://www.atmos-chem-phys.net/9/207/2009.

Schroeder, W. H., and Munthe, J.; Atmospheric mercury - an overview, Atmos. Environ., 32, 809-822, 1998.

Schwesig, D., and Matzner, F.: Pools and fluxes of mercury and methylmercury in two forested catchments in Germany, Sci. Total Environ., 260, 213-223, 2000.

Selvendiran, P., Driscoll, C. T., Montesdeoca, M. R., and Bushey, J. T.: Inputs, storage, and transport of total and methyl mercury in two temperate forest wetlands, J. Geophys. Res., 113, G00C01, doi:10.1029/2008JG000739, 2008

Sheehan, K. D., Feranadez, I. J., Kahl, J. S., and Amirbahman, A.: Litterfall mercury in two forested watersheds at Acadia National Park, Maine, USA, Water Air Soil Pollut., 170, 249-264, 2006.

Shetty, S. K., Lin, C. J., Street, D. G., and Jang, C.: Model estimate of mercury emission from natural sources in East Asia, Atmos. Environ., 42, 8674-8685, 2008.

Sigler, J. M., Mao, H., and Talbot, R.: Gaseous elemental and reactive mercury in southern New Hampshire, Atmos. Chem. Phys., 9, 1929-1942, 2009, http://www.atmos-chem-phys.net/9/1929/2009.

St. Louis, V. L., Rudd, W. M, Kelly, C. A., Hall, B. D., Rolfhus, K. R., Scott, K. J., Lindberg, S. E., and Dong, W. J.: Importance of the forest canopy to flux of methylmercury and total mercury to boreal ecosystems, Environ. Sci. Technol., 35, 3089-3098, 2001.

Stamenkovic, J., and Gustin, M. S.: Nonstomatal versus Stomatal Uptake of Atmospheric mercury, Environ. Sci. Technol. 43, 1367-1372, 2009.

Street, D. G., Hao, J. M., Wu, Y., Jiang, J. K., Chan, M., and Tian, H. Z.: Anthropogenic mercury emission in China, Atmos. Environ., 39, 7789–806, 2005.

Tekran: Model 2527A mercury vapor analyzer user manual, Toronto, Canada, 2002.

Travnikov, O.: Contribution of the intercontinental atmospheric transport to mercury pollution in the Northern hemisphere, Atmos. Environ., 39, 7541-7548, 2005.

US EPA: Method 1631: Revision B, Mercury in water by Oxidation, Purge and Trap, and Cold Vapor atomic Fluorescence Spectrometry, United States Environmental Protection Agency pp. 1-33, 1999.

US EPA: Method 1630: Methyl mercury in water by distillation, aqueous ethylation, purge and trap, and CVAFS. U.S. Environmental Protection Agency, Office of Water, Office of Science and Technology Engineering and Analysis Division (4303), 1200 Pennsylvania Avenue NW, Washington, D.C. 20460 pp. 1-41, 2001.

Valente, R. J., Shea, C., Humes, K. L., and Tanner, R. L.: Atmospheric mercury in the Great Smoky Mountains compared to regional and global levels, Atmos. Environ., 41, 1861-1873, 2007.

Wan, Q., Feng, X. B., Julia, L., Zheng, W., Song, X. J., Han, S. J., and Xu, H.: Atmospheric mercury in Changbai Mountain area, northeastern China— Part1: The seasonal distribution pattern of total gaseous mercury and its potential sources, Envrion. Res., 109, 201-206, 2009a.

Wan, Q., Feng, X. B., Julia, L., Zheng, W., Song, X. J., Li, P., Han, S. J., and Xu, H.: Atmospheric mercury in Changbai Mountain area, northeastern China II. The distribution of reactive gaseous mercury and particulate mercury and mercury deposition fluxes, Envrion. Res., 109, 721-727, 2009b.

Wang, Y. Q, Zhang, X. Y., and Draxler, R. R.: TrajStat: GIS-based software that uses various trajectory statistical analysis methods to identify potential sources from long-term air pollution measurement data, Environ. Model. Soft., 24, 938-939, 2009.

Wang, Z. W., Zhang, X. S., Xiao, J. S., Ci, Z. J., and Yu, P. Z.: Mercury fluxes and pools in three subtropical forested catchments, southwest China, Environ. Pollut., 157, 801-808, 2008.

Witt, E. L., Kolka, R. K., Nater, E. A., and Wickman, T. R.: Influence of the forest canopy on total and methyl mercury deposition in the boreal forest, Water Air Soil Pollut., 199, 3-11, 2009.

Wu, Y., Wang, S. X., Streets, D. G., Hao, F. M., Chan, M., and Jiang, J. K.: Trends in Anthropogenic Mercury Emissions in China from 1995 to 2003, Environ. Sci. Technol., 40, 5312-5318, 2007.

Zhang, H. H., Poissant, L., Xu, X. H., and Pilote, M. : Explorative and innovative dynamic flux bag method development and testing for mercury air–vegetation gas exchange fluxes, Atmos. Environ., 39, 7481-7493, 2005.

Table 1 Statistical summary of THg and MeHg concentrations and deposition fluxes in precipitation, throughfall and litterfall

	Rainfall depth (mm)	Concentration		Annual deposition flux	
		THg (ng L^{-1})	MeHg (ng L^{-1})	THg (μg m^{-2} yr^{-1})	MeHg (μg m^{-2} yr^{-1})
Precipitation	1533	4.0 (n=31)	0.04 (n=28)	6.1	0.06
Throughfall	1182	8.9 (n=31)	0.10 (n=25)	10.5	0.12
Litterfall	Litter Mass (g m^{-2} yr^{-1})	THg (ng g^{-1})	MeHg (ng g^{-1})	THg (μg m^{-2} yr^{-1})	MeHg (μg m^{-2} yr^{-1})
Cinnamomum camphora (L.) Presl	287	106	0.80	30.4	0.23
Rhododendron simsii Planch	308	57	0.44	17.6	0.14
Fargesia spathacea Franch	642	110	0.72	70.6	0.46

Table 2 Seasonal statistical summary of GEM concentrations, direct wet deposition and net throughfall deposition fluxes of THg and MeHg in Mt. Leigong

	GEM (ng m^{-3})			Direct wet deposition (ng m^{-2} mon^{-1})		Net throughfall deposition(ng m^{-2} mon^{-1})	
	Geomean	SD	Range	THg	MeHg	THg	MeHg
Spring	3.21	1.20	1.05-12.6	664	6.8	553	11
Summer	1.88	1.21	0.41-12.9	885	9.1	722	5.0
Autumn	2.85	1.60	0.41-23.9	192	1.6	180	6.2
Winter	3.59	1.54	0.85-17.5	212	3.8	54	-0.4

Figure 1

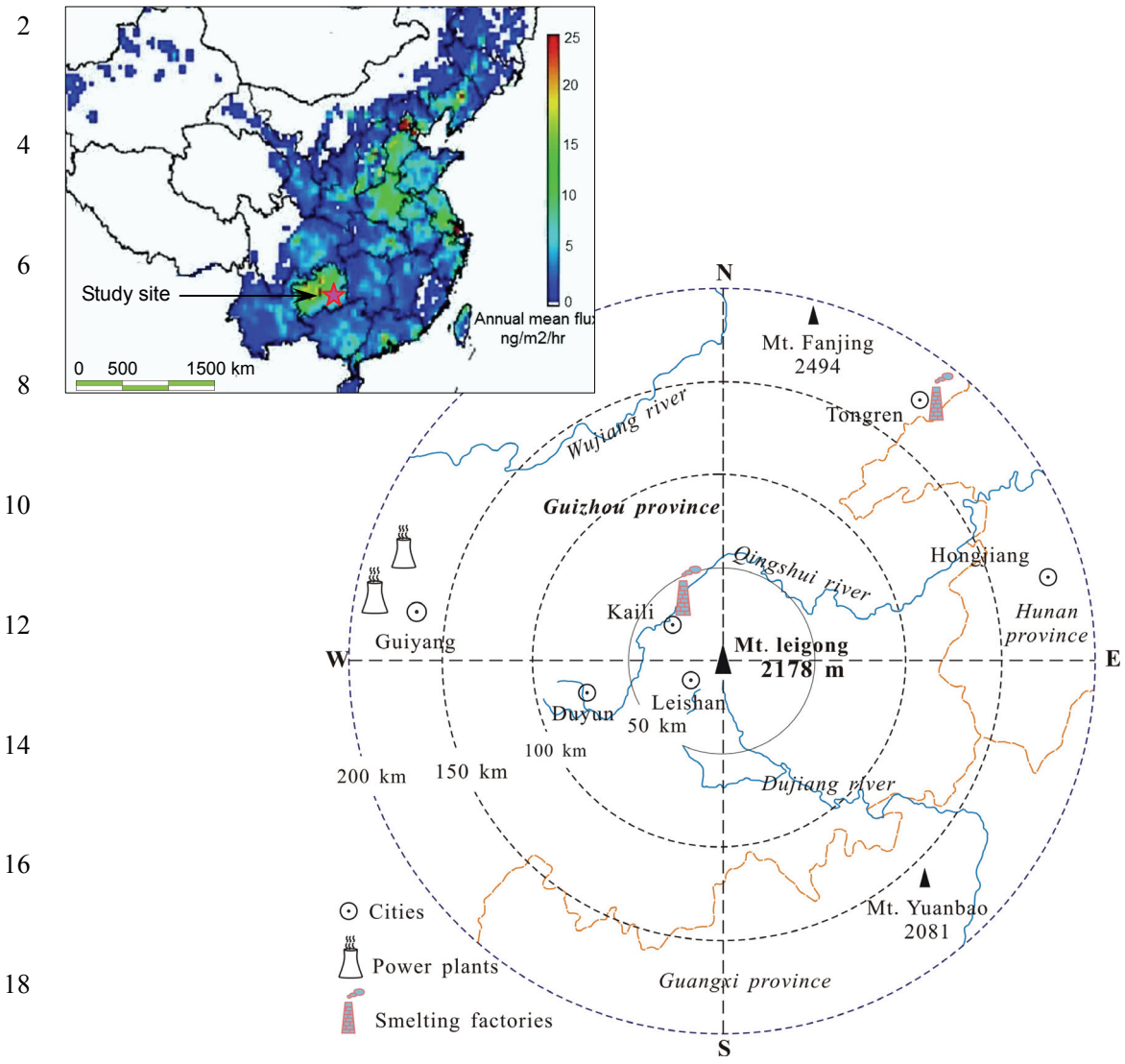
Study site
0 500 1500 km
25
20
15
10
5
0
Annual mean flux
ng/m2/hr
N
S
W
E
Mt. Fanjing
2494
Tongren
Wujiang river
Guizhou province
Qingshui river
Hongjiang
Hunan
province
Kaili
Guiyang
Mt. leigong
2178 m
Duyun
Leishan
50 km
100 km
150 km
200 km
Dujiang river
Mt. Yuanbao
2081
Cities
Power plants
Smelting factories
Guangxi province

Figure 2

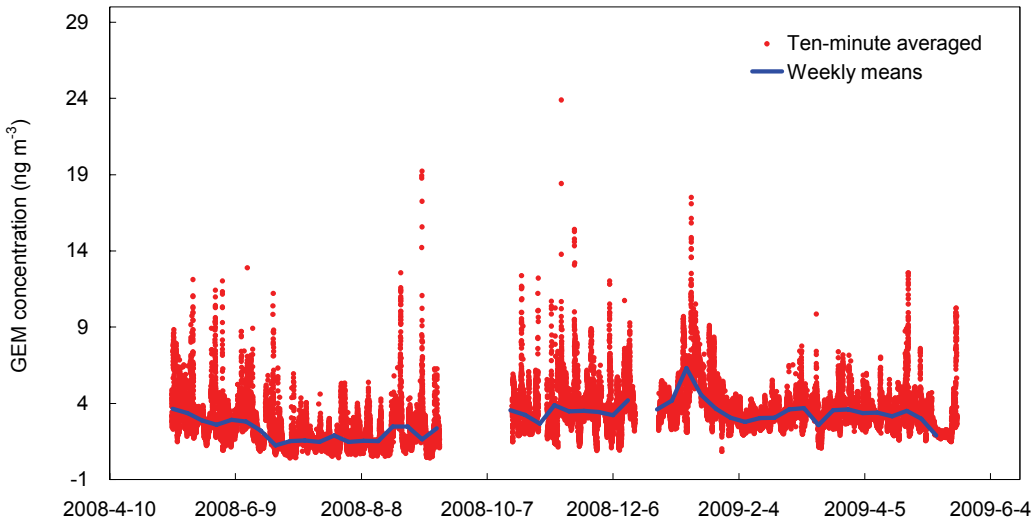
Ten-minute averaged
Weekly means
GEM concentration (ng m-3)
29
24
19
14
9
4
-1
2008-4-10
2008-6-9
2008-8-8
2008-10-7
2008-12-6
2009-2-4
2009-4-5
2009-6-4

Figure 3

2

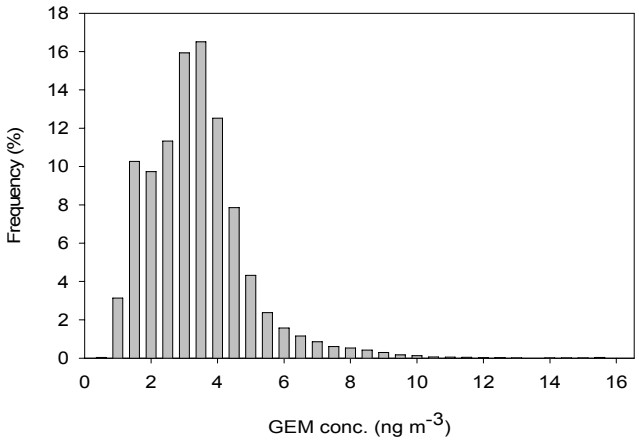

4

Figure 4

2

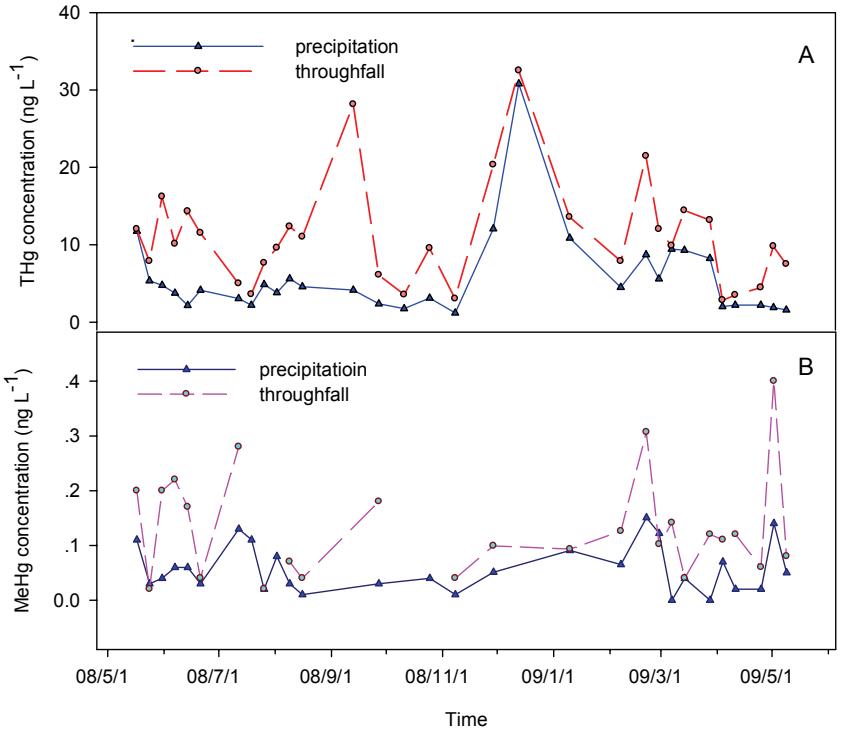
precipitation
throughfall
A
THg concentration (ng L-1)
40
30
20
10
0
precipitatioin
throughfall
B
MeHg concentration (ng L-1)
.4
.3
.2
.1
0.0
08/5/1
08/7/1
08/9/1
08/11/1
09/1/1
09/3/1
09/5/1
Time

4

Figure 5

2

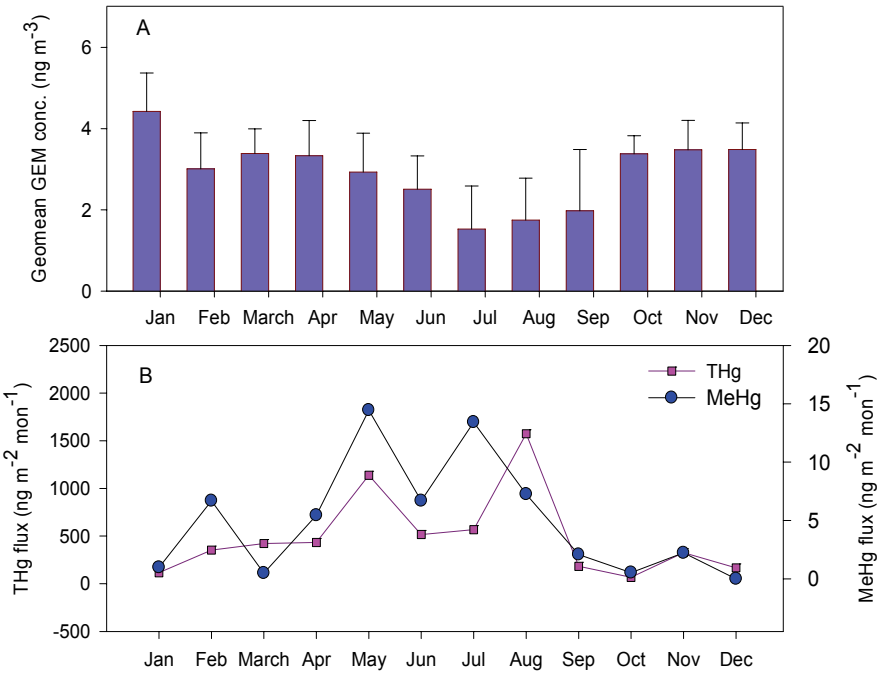
A
Geomean GEM conc. (ng m-3)
0
2
4
6
Jan
Feb
March
Apr
May
Jun
Jul
Aug
Sep
Oct
Nov
Dec
B
THg
MeHg
THg flux (ng m-2 mon-1)
MeHg flux (ng m-2 mon-1)
-500
0
500
1000
1500
2000
2500
0
5
10
15
20

4

Figure 6

2

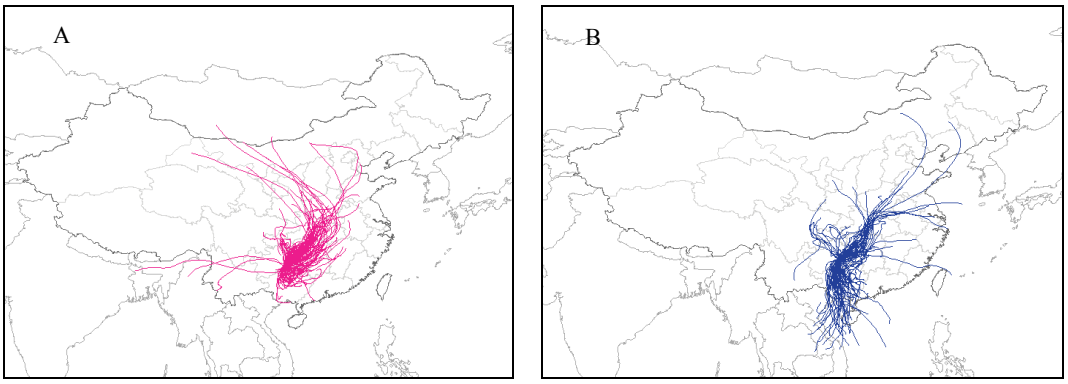

4

Figure 7

2

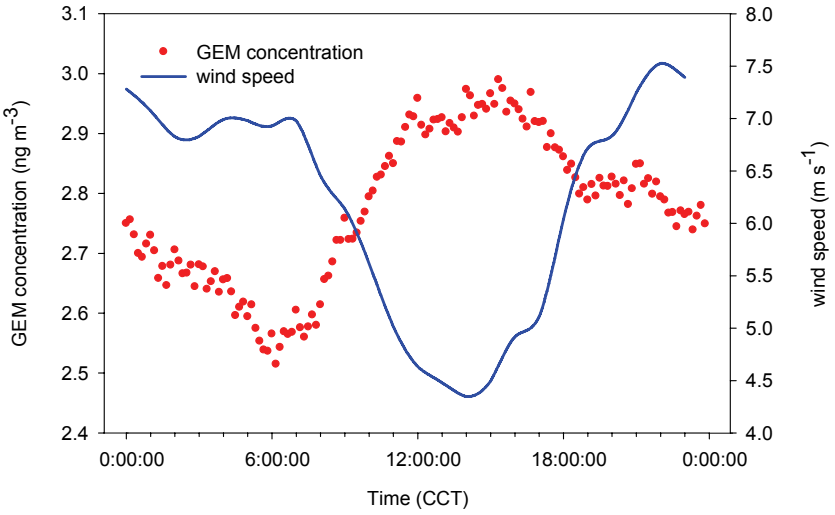
GEM concentration
wind speed
GEM concentration (ng m-3)
wind speed (m s-1)
Time (CCT)
3.1
3.0
2.9
2.8
2.7
2.6
2.5
2.4
8.0
7.5
7.0
6.5
6.0
5.5
5.0
4.5
4.0
0:00:00
6:00:00
12:00:00
18:00:00
0:00:00

4

Figure 8

2

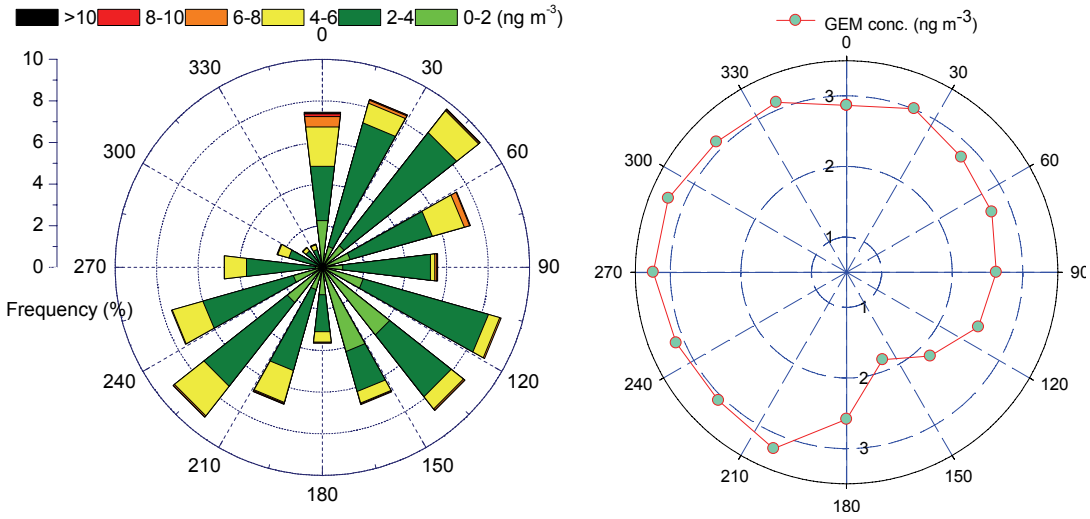
>10
8-10
6-8
4-6
2-4
0-2 (ng m-3)
0
30
60
90
120
150
180
210
240
270
300
330
10
8
6
4
2
0
Frequency (%)
GEM conc. (ng m-3)
3
2
1

4

Figure 9

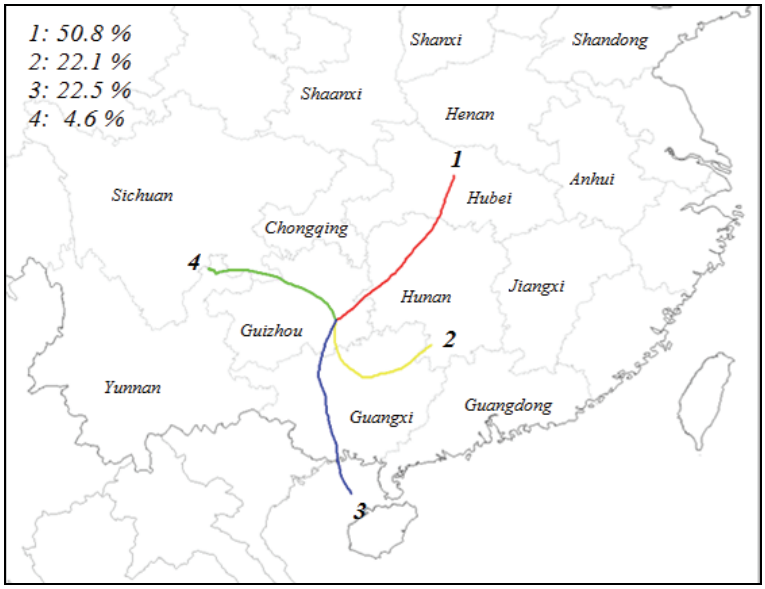
1: 50.8 %
2: 22.1 %
3: 22.5 %
4: 4.6 %
Shanxi
Shandong
Shaanxi
Henan
1
Anhui
Sichuan
Hubei
Chongqing
4
Hunan
Jiangxi
Guizhou
2
Yunnan
Guangdong
Guangxi
3

2

4